



Reverse osmosis membrane performance for desalination of Algerian brackish water

Abderrezak Bouchareb^a, Mehdi Metaiche^a, Hakim Lounici^{b,*}, Hakim Djafer Khoudja^a, Abdelwahab Lefkir^c, Nadjib Drouiche^d

^aLaboratory of Energy, Water, Environment, PM3E, Bouira University, Algeria, Campus Pole Technologique, 1000, Bouira, Algeria, emails: a.bouchareb@univ-bouira.dz (A. Bouchareb), metiche022000@yahoo.fr (M. Metaiche), djefrehyd@yahoo.fr (H.D. Khoudja)

^bLaboratory MDD, Bouira University, Campus Pole Technologique, 1000, Bouira, Algeria, Tel. +213 21 279880 Ext. 192; Fax: +213 21 433511; emails: hakim_lounici@yahoo.ca, najibdrouiche@yahoo.fr

^cLaboratory of TPiTE, ENSTP, Algiers, Algeria. BP 32, Rue Sidi Garidi, Kouba, Alger, Algeria, email: a_lefkir06@yahoo.fr

^dCentre de Recherche en Technologie des Semi-conducteurs pour l'Energétique (CRTSE), 2, Bd Dr. Frantz Fanon P.O. Box 140, Algiers-7 mervilles, Algiers 16038, Algeria, email: najibdrouiche@yahoo.fr

Received 15 October 2017; Accepted 3 February 2019

ABSTRACT

Desalination of brackish water (BW) is an effective approach to increase water supply, especially for inland regions that are far from seawater resources. Reverse osmosis (RO) is currently one of the most widely used methods of desalination in the world and widely used. The membranes used in the RO process play a vital role in determining the effectiveness of the desalination process depending on the water qualities feeds. Algeria represents the largest country in Africa characterized by two major regions the Alpine region in the north and the Saharan platform in the south. The purpose of this paper is to give an overview of the desalination process by assessing the performance of RO polyamide thin-film composite membrane (TW30-2540) purchased from Dow Chemical Company in terms of water permeability, salt permeability, selectivity and mass transfer coefficient using three different brackish water sources from the Alpine region. These regions are characterized by the high salinity of water. In conclusion, our study showed that TW30.2540 membrane could be used for desalination of brackish water with less cost compared with the currently used membranes BW30.2540, XLE 2540. The TW30.2540 membrane removed efficiently (97%) the salts referred by the total dissolved salt.

Keywords: Reverse osmosis (RO); Permeability of pure water (A); Permeability of salts (B); Mass transfer coefficient (k); Salt rejection (R)

1. Introduction

Less than one percent of all freshwater on earth is usable by humans. Most freshwater is inaccessibly locked into polar ice caps or permanent mountain snow cover. Freshwater as a whole constitutes only 2.5% of Earth's water—the vast majority is saltwater (97%) from the seas and oceans, and the small remainder is brackish water (0.5%) found in surface estuaries and salty underground aquifers. From the freshwater that is accessible to humans, 70% is used for

irrigation, 20% is allocated for the industry, and only 10% is for domestic use. The latter figure is not enough since 1.2 billion people worldwide do not have access to safe drinking water and 2.6 billion lacks inadequate sanitation [1].

With an ever-expanding global population and growing industrial capacity, access to clean water is due to become an increasingly critical issue, both for creating safe drinking water and in the provision of adequate supplies for agricultural and industrial consumption. Recent projections

* Corresponding author.

suggest as many as 3.9 billion people worldwide are expected to be living in severe water-stressed areas by 2030 [2].

Last centuries have witnessed significant accelerated anthropogenic changes in the earth-atmospheric system due to numerous factors like (1) rapid industrialization, (2) population increase, (3) higher-energy use and (4) change in land usage. Driven by these changes, the climatic system of the globe is showing signs of persistent changes that are increasing with time [3].

The most well-established cause is that of the global increase in temperature. During the period of 1920 to 2000, the temperature has increased about 0.1°C per decade and it is predicted that by 2050s the temperature may increase between 1.5°C – 3.5°C , and precipitation decrease in most territories (about 10%–20% decrease depending on the season in the 2050s). A small increase in temperature can seriously disrupt the natural balance of the world's climate and thus result in change of water cycle [3,4]. Water quality nowadays needs more attention and serious treatment.

In fact, water and energy are strongly linked to each other. Cogeneration of water and power is a common practice especially in the Middle East and North African (MENA) countries [5].

Algeria is characterized by a semi-arid climate that brings a high degree of scarcity in water availability (the rivers dry frequently). The average theoretical availability of water has reached a critical threshold estimated at $500\text{ m}^3\text{ cap}^{-1}\text{ y}^{-1}$. This threshold represents less than half the scarcity threshold fixed by the World Bank at $1,000\text{ m}^3\text{ cap}^{-1}\text{ y}^{-1}$, and less than the fifth of the threshold of $2,000\text{ m}^3\text{ cap}^{-1}\text{ y}^{-1}$ [6]. The reserves of groundwater in Algeria are estimated to 6.8 billion m^3 ; however, these groundwaters are at significant depths and are characterized by a strong mineralization (Fig. 1) [7].

Desalination is used to separate salts from raw water for use in boiler feed, thermal power generation, electronic industries, chemical industries, textile industries, leather industry and for the production of drinkable water. The process is carried out through distillation, multiple effect vapor compression, evaporation, or membrane processes such as electro dialysis reversal, nanofiltration, and reverse osmosis (RO) [9].

Desalination of seawater or brackish water is one of the technologies that have been introduced to remove salt and other minerals from saline and salty water to make it suitable for human consumption or industrial use. The desalination of water is split between sea water representing 58.9% and brackish groundwater representing 21.2%. The remaining percentage is from surface water and saline wastewater.

The increase of desalination capacity is caused primarily not only by increase in water demand but also by the significant reduction in desalination cost due to the significant advance in technology that resulted in making desalinated water cost-effective with other water sources. In some specific areas, desalination has now been able to successfully compete with conventional water resources and water transfers for potable water supply [10,11].

Membrane processes in aqueous applications can be grouped according to the applied driving forces:

- (1) pressure-driven processes, namely micro-, ultra-, and nanofiltration as well as reverse osmosis,
- (2) concentration-driven processes, namely dialysis and

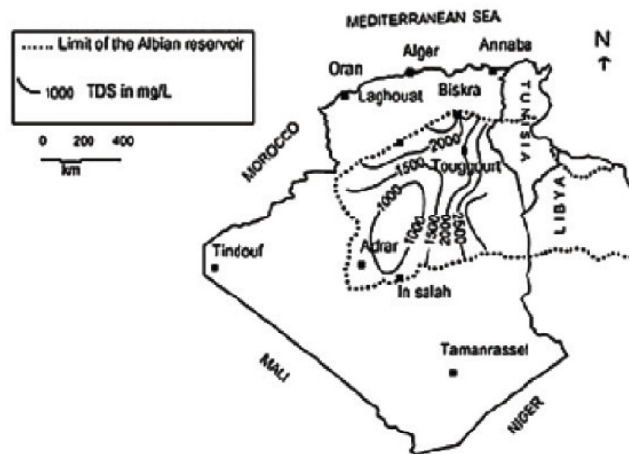


Fig. 1. Distribution of total dissolved solid concentrations (TDS) in groundwater from the Albian reservoir (in mg L^{-1}) in Southern Algeria [8].

forward osmosis, (3) processes driven by an electrical potential, i.e., electro dialysis, (4) processes driven by partial pressure and vapor pressure, namely pervaporation and membrane distillation, and final (5) processes driven by differences in chemical potential, for example, Supported liquid membranes, membrane contactors, and membrane reactors [12]; Another technique with a significant potential for energy efficient water desalination specially for brackish water using a porous carbon electrodes is the capacitive deionization (CDI) technique. In this technique, salt ions are removed from brackish water upon applying an electrical voltage difference between two porous electrodes. The ions will be temporarily immobilized. These electrodes are made of porous carbons optimized for salt storage capacity and ion and electron transport [13].

In the recent years, RO membrane technology became the leading technology for new desalination installations and has developed for both brackish and seawater applications. Brackish water RO membranes typically have higher product water flux, lower salt rejection, and require lower operating pressures due to lower osmotic pressure [12,14]. Brackish water RO plants tend to be smaller in production capacity than seawater RO plants. A greater number of brackish water RO plants (48% of the total number of plants) are in operation worldwide compared with seawater RO plants (25%). The remaining desalination plants (27%) consist of other feed waters, including rivers, wastewater, and pure water [15].

The main objective of this paper is to give an overall understanding of brackish water desalination in Algeria. The performances of RO seawater commercial membrane Filmtec TW30.2540 using three samples of brackish water from two regions (Bouira and Setif) located in the east of Algeria were determined. These regions suffer from the high salinity of water quality. Our results were compared with results obtained from the literature for two other membranes from the same manufacturer the BW30.2540 and the XLE.2540. They gave an insight into the efficiency of RO technique facing water shortage in Algeria.

2. Reverse osmosis background

Water and salt fluxes via the membrane is estimated by Kimura–Sourirajan model [16]:

$$J_w = A_w \cdot (\Delta p - \Delta(\pi_m - \pi_p)) \quad (1)$$

$$J_s = A_s \cdot (C_m - C_p) \quad (2)$$

where ΔP represents the pressure difference between the high concentration side and low concentration side of the membrane. The subscripts w, m, p, s refer to water, membrane surface, permeate and solute, respectively.

The volume and mass balance equations around the spiral wound element are given by:

$$Q_f = (Q_r + Q_p) \quad (3)$$

$$C_f \cdot Q_f = (C_r \cdot Q_r + C_p \cdot Q_p) \quad (4)$$

The water permeate concentration and flow is expressed as:

$$C_p = (J_s / J_w) \quad (5)$$

$$Q_p = (S \cdot J_w) \quad (6)$$

The recovery (Y) is defined as the fraction of the feed flow which passes through the membrane:

$$Y = Q_p / Q_f = A_w \cdot S \cdot (\Delta p - (\pi_m - \pi_p)) / Q_f \quad (7)$$

where S is the active area of the membrane = 2.6 m².

The separation efficiency of an RO membrane for a given solute is expressed by the rejection coefficient r_j :

$$r_j = (1 - C_p / C_f) = ((C_f - C_p)) / C_f \quad (8)$$

The permeate flux cannot be known unless the membrane wall concentration is known. At the same time, this concentration needs the value of water flux to be evaluated. Therefore, an iterative calculation is needed. Concentration polarization on membrane surface phenomenon may be described using the film theory [17] as function of mass transfer coefficient:

$$C_p = (C_m - C_p) / (C_b - C_p) = \exp(J_w / k) \quad (9)$$

2.1. Sherwood correlation

One dimension laminar flow and one dimension turbulent flow are estimated by this expression [18]:

Laminar flow:

$$Sh = 1.66 \cdot Re^{0.36} \cdot Sc^{0.34} \cdot (dh/L)^{0.42} \quad (10)$$

Turbulent flow:

$$Sh = 0.073 \cdot Re^{0.74} \cdot Sc^{0.34} \cdot (dh/l)^{0.32} \quad (11)$$

3. RO pre-treatment

The primary goal of any RO pre-treatment system (for seawater or brackish water) is to lower the fouling tendency of the water in the RO membrane system. Surface water resources (Seawater and brackish water) typically have a more significant tendency for membrane fouling and require more extensive pre-treatment systems than groundwater resources [15]. In general, seawater RO tends to use surface water sources, while brackish water RO often uses groundwater sources.

It should be noted that though the pre-treatment system has the largest share of the burden of fouling prevention, the RO system design also plays an important role. Fouling is traditionally defined as a decline in permeate due to accumulation of insoluble rejected matter on membrane surface; For instance, RO system designs that enable high cross flow velocities relative to RO flux can minimize effects of many fouling problems. There are five distinct types of membrane fouling where the pre-treatment system may be required to mitigate [19–21], these include:

1. Particulate fouling generally refers to fouling by suspended particles in water it will build up as a physical occlusion on the membrane surface and feed spacer. Particulate fouling is most severe in the lead RO elements in the pressure vessels. This type of fouling is usually easily mitigated by improving the coagulation/flocculation/filtration steps in the pretreatment system.
2. Colloidal fouling particles in the range of 1 nm to 1 μ m which results in a loss of permeate flux through the membrane.
3. Scaling which is defined as the formation of minerals deposits precipitating from feed stream onto the membrane surface.
4. Bio-fouling represents the “Achilles heel” of the membrane process because microorganisms can multiply over time; even if 99.9% of them are removed, there will be still enough cells remaining which can continue to grow at the expense of biodegradable substances in the feed water.
5. Organic fouling due to the deposition of organic substances.

4. Methods and materials

4.1. Feed water characteristic

The feed water coming from three different wells from south east of Algeria, one from the town of Setif and the other two from a town of Bouira located 150 and 80 km respectively

from the sea; We noted that the conductivity increased from feed I > feed III > feed II, and the turbidity increased from feed II > feed I > feed III.

The characteristics of the feed water are given in Table 1.

4.2. Reverse osmosis pilot

A multi-cellular centrifugal pump high pressure (16 bar with a maximum flux of 800 L h⁻¹) feeds a circuit including a reverse osmosis cartridge. This circuit consists of a power supply, a discharge and permeate. The tank has a capacity of 100 L for the treatment of solution and the drip tray has a capacity of 20 L. They are both PVC transparent. The feed tank is filled with a 25 µm filter and an active carbon filter (5 µm). Anyone can operate independently the system from the input tray. The pump stops automatically when the low level of the tank is reached (Fig. 2).

Table 1
Feed water characteristics

Characteristic	Feed I	Feed II	Feed III
pH	7.75	6.95	7.05
Temperature °C	17	19	19
Conductivity (mS cm ⁻¹)	6.46	3.77	4.65
TDS (mg L ⁻¹)	3,852	2,262	2,790
Turbidity (NTU)	1.2	4.35	0.93
Calcium (mg L ⁻¹)	560.88	228	280
Sodium (mg L ⁻¹)	1,360	680	1,020
Magnesium (mg L ⁻¹)	106.27	43.20	54.72
Potassium (mg L ⁻¹)	1.42	15.90	2.10
Chloride (mg L ⁻¹)	2,680	1,340	2,000
Bicarbonate (mg L ⁻¹)	549	427	219.6
Sulfate (mg L ⁻¹)	85	85	98
carbonate (mg L ⁻¹)	0.53	0.33	1.66

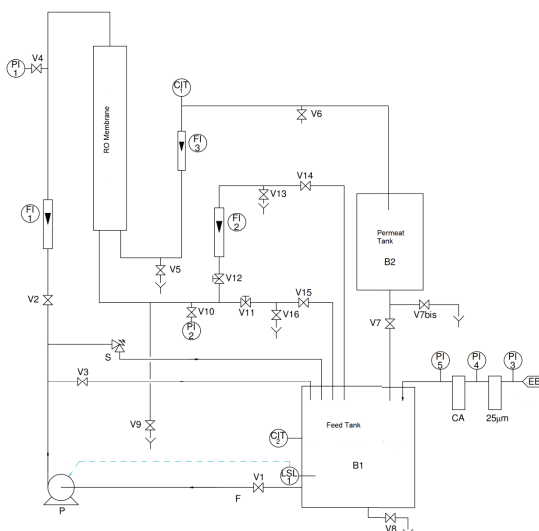


Fig. 2. Schematic diagram of reverse osmosis MP20 device.

List of instrumentation and controls included in the system are presented in Table 2.

4.3. Reverse osmosis membrane

The RO type cartridge membrane used in this study was provided by DOW Chemical Company (Dow-Filmtec, TW30-2540); The membranes are spiral wound modules each with a surface area of 2.6 m² allowing a permeate flow of 3.2 m³ d⁻¹ with a salt rejection of 99.5%; The operating characteristics of the membrane are shown below in Table 3 [22].

4.4. Jar test coagulant/flocculants experiments

A pretreatment is an important step before using RO membrane to increase the life span and to protect the RO membrane sheet from any kind of fouling. In this study we conducted a conventional pretreatment based on coagulation/flocculation/sand filter; To get the conditions that will be utilized in this pretreatment, few tests will be performed using DAIHAN Wise mix JT-M6 Digital Jar Tester, To analyze all data we took into consideration the sample used of one liter of water, the ferric chloride hexa-hydrate (FeCl₃·6H₂O) and cationic polymer (bentonite) from (Chema-Pharma) Canada.

Table 2
List of instrumentation

Purpose	Manufacturer	Model number
Pump	Lowara	e-SV K 3
Flow	Bamo	PDP/731
Pressure	Baumer	D100-MEX5
Conductivity and temperature	Endress+Hauser	M CLM 223

Table 3
Sheet TW30-2540 membrane characteristic

Membrane type	Polyamide thin-film composite
Maximum operating temperature ^a	3°F (45°C)
Maximum operating pressure	600 psig (41 bar)
Maximum feed flow rate	6 gpm (1.4 m ³ hr ⁻¹)
Maximum pressure drop	13 psig (0.9 bar)
pH range, continuous operation	2–11
pH range, short-term cleaning (30 min.) ^b	1–13
Maximum feed silt density index	SDI 5
Free chlorine tolerance ^c	< 0.1 ppm

^aMaximum temperature for continuous operation above pH 10 is 95°F (35°C).

^bRefer to Cleaning Guidelines in specification sheet 609-23010.

^cUnder certain conditions, the presence of free chlorine and other oxidizing agents will cause premature membrane failure.

We prepared six Jars of one liter from the water sample into the tester stirring at 200 rpm. At time $t = 0$ s we added the coagulant at different concentrations to each jar. After 3–5 min, we reduced the speed to 60 rpm and added the polymer with different concentrations to each jar; after 30 min at 60 rpm stirring we stopped and we allowed a settling time after we measured the different parameters.

The optimum system for the feed I was (7 mg FeCl_3 + 0.2 mg bentonite), Feed II was (23 mg FeCl_3 + 1.1 mg bentonite), Feed III was (10 mg FeCl_3 + 0.7 mg bentonite) as function of the initial turbidity (Fig. 3).

5. Results and discussion

5.1. Hydraulic permeability

Measuring the hydraulic permeability of the membranes will allow knowing the fluxes for the feed of brackish water. In Fig. 4, we have reported the water flux as a function of the trans-membrane pressure, to calculate the water permeability we chose a pure water to run the pilot. In the case of salt permeability we worked with synthetic water in with a concentration of 3 g l^{-1} NaCl (which is typical of synthetic brackish water).

As illustrated in Fig. 4, both permeability of pure water and salt for the membrane TW30-2540 after extrapolating the water flux against the trans-membrane pressure were measured. The pure water permeability was found around $A_w = 8.3 \times 10^{-12} \text{ m.s}^{-1}.\text{pa}^{-1}$; as reported before by Geoffrey et al,

cited by [23]. The interval of water permeability against NaCl passage and the rejection ratio for Brackish water reverse osmosis membrane was between 1 and 10 $\text{l/m}^2.\text{h}.\text{bar}$). In our case the value was 2.99 $\text{l/m}^2.\text{h}.\text{bar}$. This value depends on the same interval.

Depending on the salt permeability of this membrane, highly concentrated water was used (3 g l^{-1} NaCl and $T = 20^\circ\text{C}$) with osmotic pressure of 250 kPa. Using the same method, the pure water permeability with salt permeability of $A_s = 4.19 \times 10^{-12} \text{ m.s}^{-1}.\text{pa}^{-1}$ was found.

Compared with previous similar studies using BW30-2540 and XLE-2540, the pure water permeability was higher than what was found with our membrane TW30-2540. In case of salts permeability we found almost the same value with the BW30-2540 and TW30-2540; Table 4 summarizes the values obtained.

5.2. Evolution of the different salinity water flux

The variety of the water flux over RO operation for the three different brackish wells water with a distinction pressures are represented in Fig. 5.

For all feeds water [($\text{EC}_{\text{feed I}} = 6.42 \text{ mS cm}^{-1}$, $T_{\text{feed I}} = 17.3^\circ\text{C}$, $\pi_{\text{feed I}} = 2.85 \text{ bar}$; $\text{EC}_{\text{feed II}} = 3.77 \text{ mS cm}^{-1}$, $T_{\text{feed II}} = 19^\circ\text{C}$, $\pi_{\text{feed II}} = 1.54 \text{ bar}$ and $\text{EC}_{\text{feed III}} = 4.65 \text{ mS cm}^{-1}$, $T_{\text{feed III}} = 19^\circ\text{C}$, $\pi_{\text{feed III}} = 1.97 \text{ bar}$)] we observed a continuous decrease from the first value to the last one linked to an increase in the operation pressure as presented in the figure below;

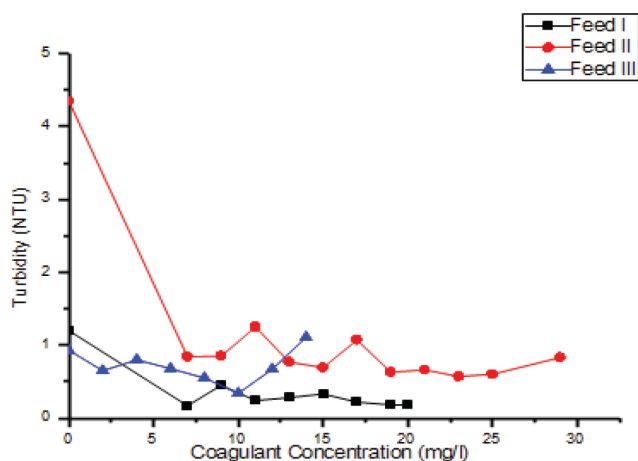


Fig. 3. Plot of turbidity progress with the corresponding of coagulant Dose (mg l^{-1}).

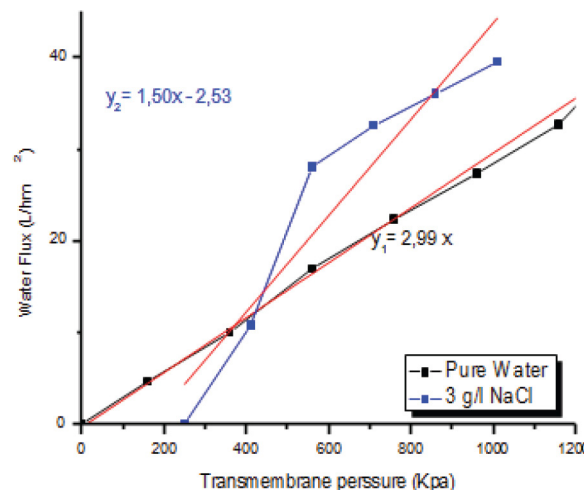


Fig. 4. Pure water and saline water flux against trans-membrane pressure.

Table 4
Permeability values of various membranes

Membrane	NaCl concentration (g L^{-1})	Water permeability ($\text{m.s}^{-1}.\text{pa}^{-1}$)	Salt permeability ($\text{m.s}^{-1}.\text{pa}^{-1}$)	Reference
BW30-540	Pure water	9.14×10^{-12}	/	[25]
TW30-540	Pure water	8.3×10^{-12}	/	This work
XLE-2540	Pure water	2.03×10^{-11}	/	[25]
BW30-540	6 g L^{-1}	/	4.16×10^{-12}	[26]
TW30-540	3 g L^{-1}	/	4.19×10^{-12}	This work

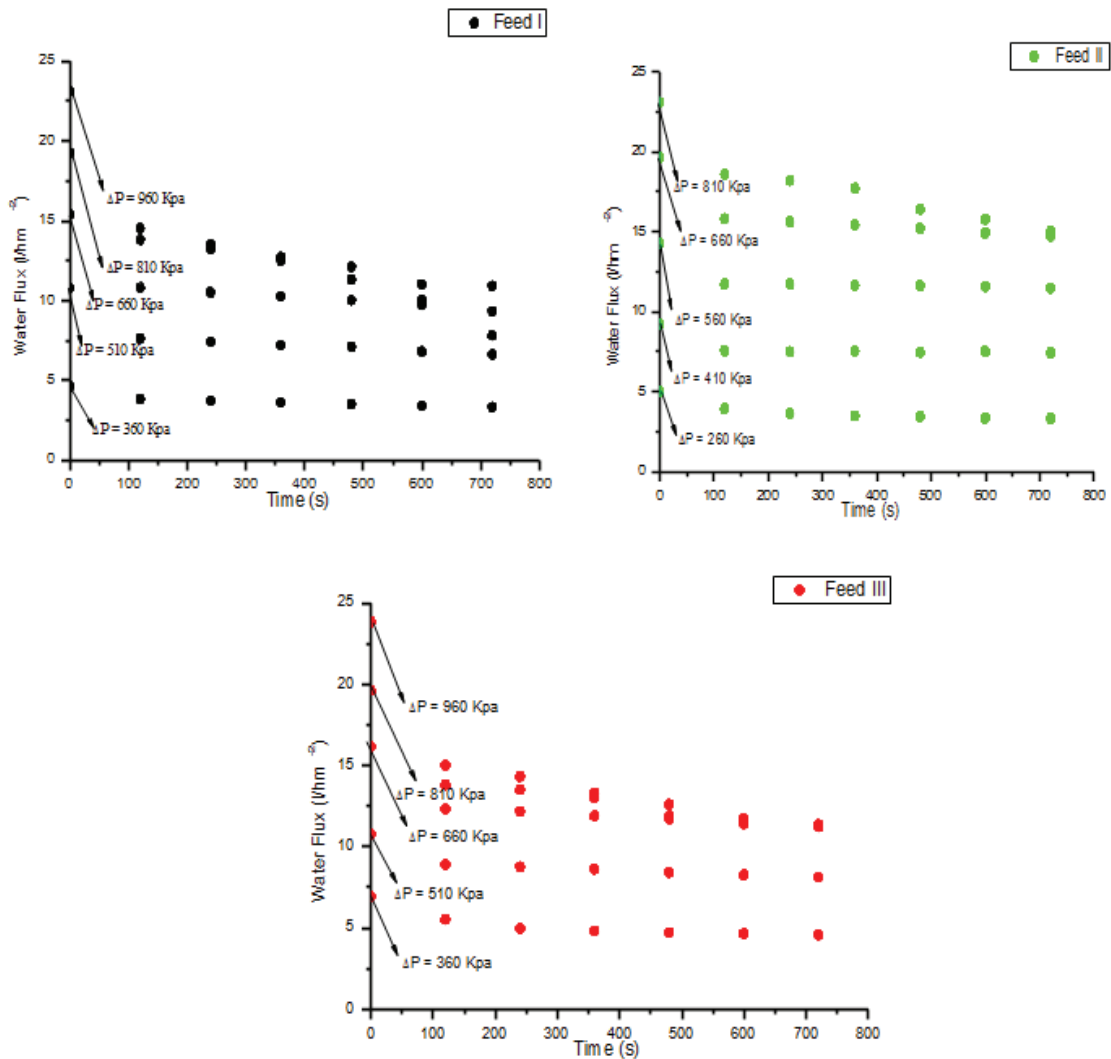


Fig. 5. Water flux obtained for three different brackish water during the RO operation for each operation pressure.

This time dependent decrease of water flux resulting from osmotic pressure effect and using batch RO was due to the treatment of both the feed and the concentrate at the same time, Eq. (1) confirmed these results. This decrease of water flux increased with time.

5.3. Chemical compoment of permeat RO water

The structure of the TW30-2540 DOW membrane was prepared by the interfacial reaction between 1,3-benzenediamine and Trimesoyl chloride producing a very unique characteristic surface called FT 30 membrane like the one in Fig. 6 [24].

The aromatic polyamide structure of FT-30 provides a high degree of thermal and chemical resistance, resistance to compression, as well as a wide pH operating range. Although, not completely resistant to chlorine attack, FT-30 shows a degree of tolerance to chlorine which is sufficient to withstand accidental exposure to this chemical [24].

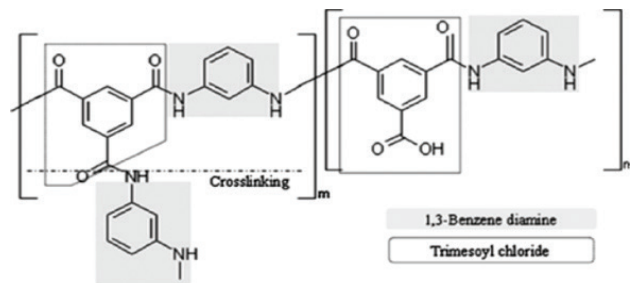


Fig. 6. FT30 DOW chemical composition [24].

In this case we treated three different brackish water with different pH ($pH_{Feed I} = 7.75$, $pH_{Feed II} = 6.95$ and $pH_{Feed III} = 7.09$). During the RO operations a decrease of permeate water pH as function of the trans-membrane pressure was observed (Fig. 7). Results are shown in Table 5.

Table 5
Evolution of pH as a function of time and operating pressure

Parameters	Feed I		Feed II		Feed III	
Time (s)	0	7,720	0	7,720	0	7,720
Pressure (KPa)	2,285	9,960	1,154	8,840	1,198	9,960
pH	7.09	6.67	6.95	5.95	7.09	5.70

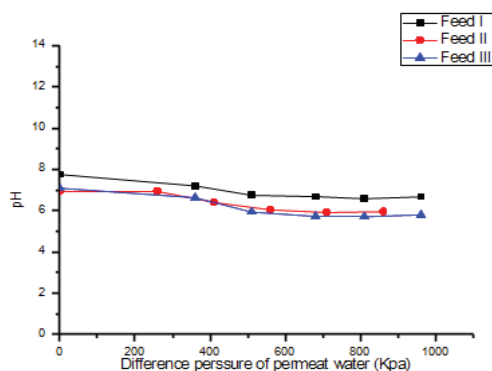
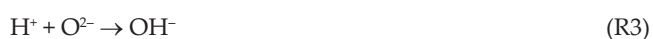


Fig. 7. Permeate pH against difference pressure operation for the three different brackish water.

The membrane surface has a saturated and stable molecule so that it has no influence to the water but only for the salt rejection. The force applied (trans-membrane pressure) by the pump for salt rejection will decrease the pH value. Among a number of salts we have the anion bicarbonate (HCO_3^-) that is decomposed following three reactions:



The RO membrane cannot reject the gases so the proton release (reaction 1) is responsible of the acidification of the permeate streams. This is more in favor of our case.

5.4. Influent of the permeate flow to the recovery rate

Evolution of the recovery rate (Y) during the RO operation is controlled by two factors the permeate flow and the feed flow. In our case a constant feed flow was applied for each operation pressure. The permeate flow can be changed with the changes in osmotic pressure like it is shown in Eq. (7). During this operation we worked with batch RO configuration. In this process the concentration increases as function of time and this increase was due to a decrease of permeate flow rate. In this study, working with three different brackish waters, we observed the same evolution of the recovery rate relative to time. For each pressure we used, we have a decrease in recovery rate.

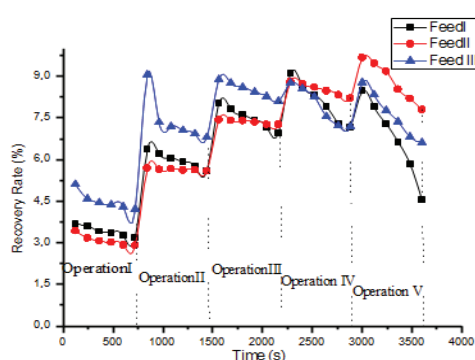


Fig. 8. Recovery rate evolution during operation time for each operation pressure.

From one operation pressure to another operation pressure the feed flow value was changed. This change was followed by a higher value of the recovery rate (Y). Fig. 8 illustrates the evolution of the recovery rate as function of the time operation for the three feed water. Because we worked with (one pass/one stage) pilot, the value of the recovery rate does not exceed 10%.

5.5. RO membrane performance in TDS rejection

The TDS concentration is widely benchmarked at 500 mg L^{-1} for the palatability of drinking water. From Eq. (8) we calculated the TDS rejection at all point during RO operation. The initial TDS of our feeds water was measured as $3852\text{--}2262\text{--}2790 \text{ mg L}^{-1}$, which represents completely brackish water, Fig. 9 represents a variation of TDS rejection during $3,600 \text{ s}$ with aid of different flow rates. There was an increase in the TDS rejection when working with a higher flow rate (Fig. 9). This could be explained by large flow rates that can enhance the mass transfer and therefore reduce the concentration polarization factor.

We have a continuous increase of the water flux as function of the salt flux like we showed in Eq. (5). For a high value of permeate concentration we got a high value of water flux (Fig. 10(a)). The permeate flow rate increase was followed by an increase in the recovery rate which was allowed by higher value of TDS rejection. The combination between Eqs. (8) and (5) can evince what we already stated (Fig. 10(b)).

5.6. Mass transfer coefficient

The expression of the mass transfer coefficient (k) changed as the flow changed with a laminar flow and the

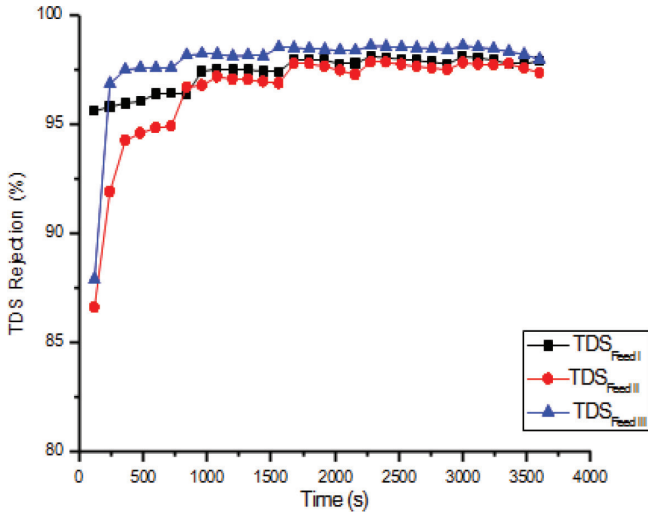


Fig. 9. TDS rejection rate with each feed flow rate during operation time.

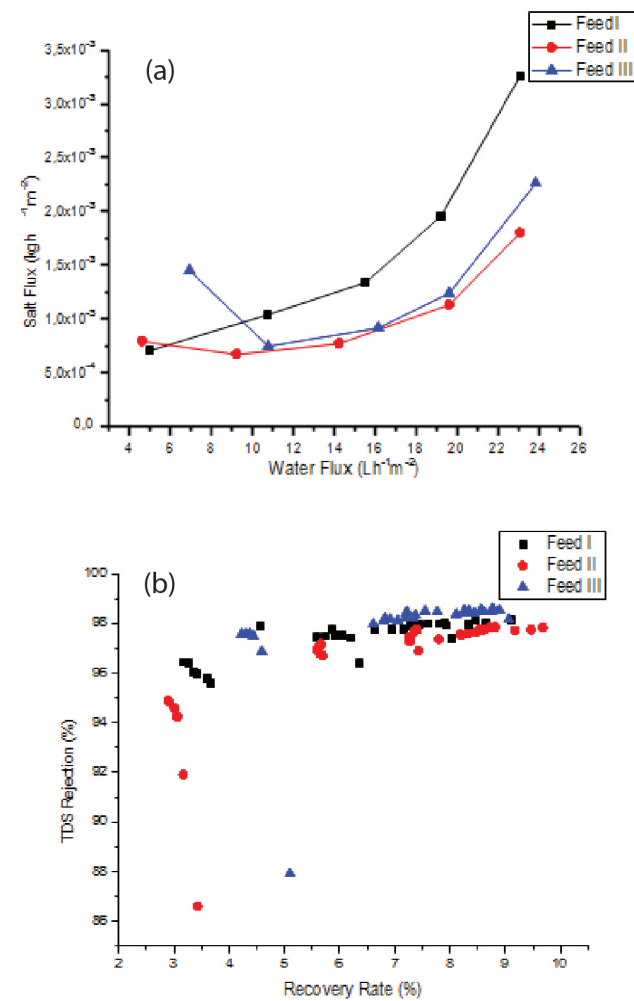


Fig. 10. (a) Corresponding salt flux against waterflux for each feed water, and (b) represent the TDS rejection against recovery rate.

turbulent flow (the equations shown in the appendix (12, 13) was used); The only parameter that can designate the type of flow is the Reynolds number (Re), if the Reynolds number (Re) is less than 2,000 the flow is laminar and if the Re number is 2,000 the flow is turbulent. In our study we work with $Re < 2000$ and a laminar flow. In this case the mass transfer coefficient (k) was calculated with aid of Eq. (12). The obtained average values of the mass transfer coefficient (k) for all the feed water was about $E(-5)$, similar with the results obtained with the BW30-2540 and XLE-2540 [25]; for $k_{feed I} = 0.923 \times 10^{-5} m s^{-1}$, $k_{feed II} = 0.7433 \times 10^{-5} m s^{-1}$ and $k_{feed III} = 0.821 \times 10^{-5} m s^{-1}$, the obtained mass transfer coefficient (k) in each point of RO operation were plotted against the corresponding diffusion coefficient (D) and time (t) in Figs. 11(a) and (b), demonstrating a clear increase of the mass transfer coefficient (k) with increasing of the diffusion coefficient (D) once and with time (t) in other hand.

Taking into consideration the Sherwood correlation, we concluded that the Sherwood number was related to two parameters the Reynold number and the Schmidt number. In our study, as we had the laminar flow we used the Eq. (10).

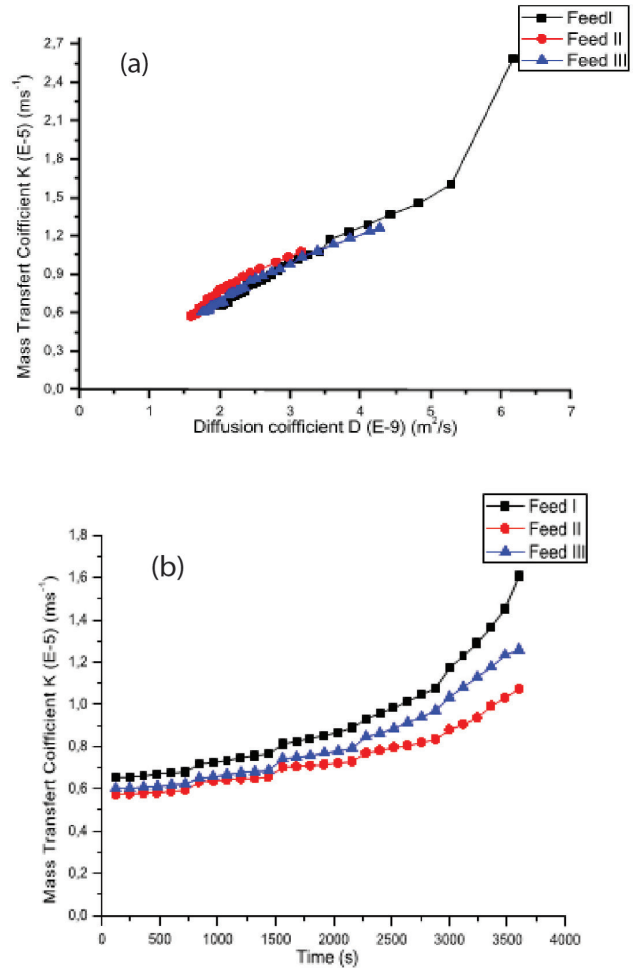


Fig. 11. (a) The mass transfer coefficient (k) against the diffusion coefficient (D) with the different water use, and (b) evolution of the mass transfer coefficient during operation time.

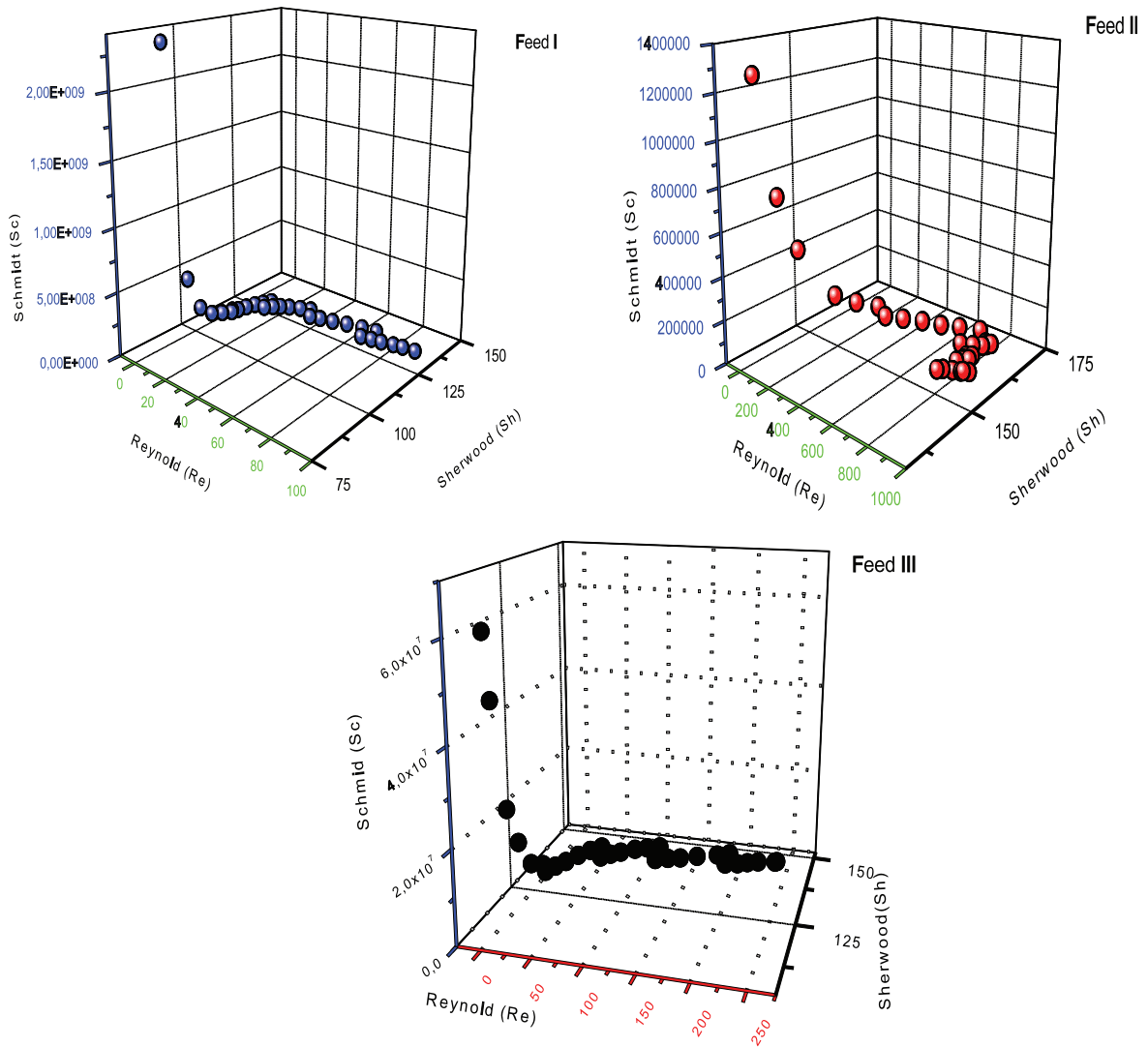


Fig. 12. Sherwood number against Reynolds number and Schmidt number for all feed waters.

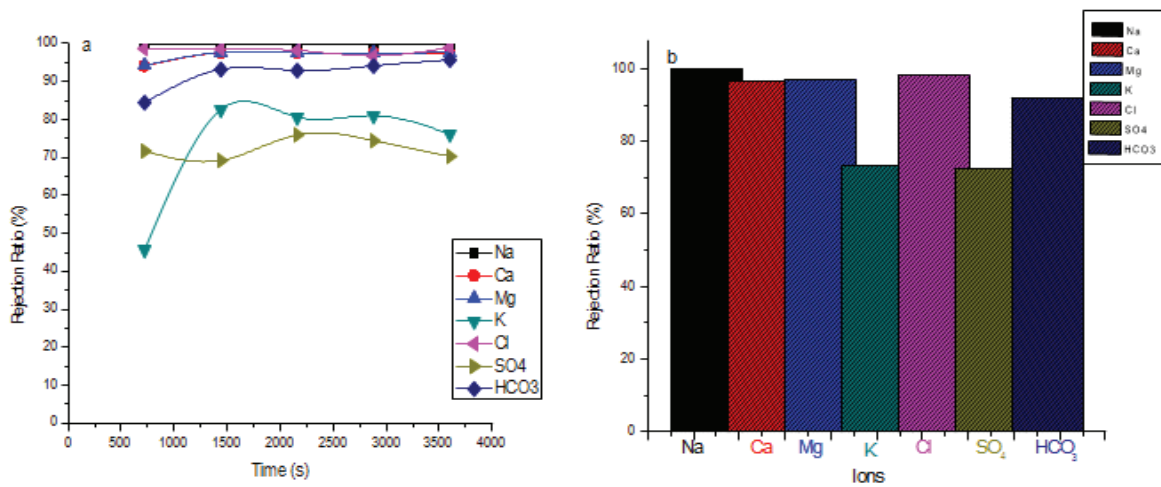


Fig. 13. Evolution of the rejection rate for each ion during RO operation.

The evolution of Sherwood number against Reynold and Schmidt numbers was studied (Fig. 12). A clear decrease of Sherwood number correlating with a decrease of Reynold number for all feed waters was observed. This was due to the low feed velocity (low feed flow) in one pass/one stage device.

5.7. A TW30-2540 performance in ions salts rejection

The rejection rate for NaCl salt is about 99.5%, for brackish water RO membrane (TW30-2540) according to the manufacturer Dow Chemical Company. In this section we measured the rejection rate for each ions salt with the aid of the Ionics analysis and the RO theoretical background (Eq. (11)). We noticed that the most ion rejected is the sodium with a value of 99.8%, followed by the chloride with 98.21% (Fig. 13). Other ions had the minimum value of rejection, like the sulfate with 72.29%, potassium with 73.17%, calcium and the magnesium had almost the same rejection rate with (96.77%, 96.88% respectively) and the bicarbonate had 92.07% rejection rate.

6. Conclusion

The main objective of this work was to compare the performance between three SW commercial membrane BW30.2540, XLE 2540 and TW30.2540 and to define the performances of the TW30.2540 membrane.

Membrane performance focused on water permeability A_w , salt permeability A_s , mass transfer coefficient k and rejection rate R . The results obtained by using three Algerian brackish water samples for desalination were as follow:

- All membranes had the same salts permeability (A_s) with differences in water permeability A_w (A_w (BW30.2540) > A_w (XLE2540) > A_w (TW30.2540)).
- Similar average for the mass transfer coefficient was obtained in our study using a laminar flow (Confirmed by $Re < 2,000$) compared with other membranes E(5).
- The TDS rejection ration tested with the membrane TW30.2540 on three different brackish water was about 97% less of what the manufacturer claims to be 99.5%.

Symbols

A_s	– Salt permeability, $m s^{-1}$
A_w	– Water permeability, $m^3 \cdot m^{-2} \cdot s^{-1} \cdot bar$
C	– Concentration, $g l^{-1}$
CP	– Concentration polarization
D	– Diffusion coefficient, $m^2 s^{-1}$
d_h	– Hydraulic diameter for channel flow, m
f	– Feed
h	– Feed channel height
J_s	– Salt flux, $kg \cdot m^{-2} \cdot s^{-1}$
J_w	– Water flux, $l h^{-1} \cdot m^{-2}$
k	– Mass transfer coefficient, $m s^{-1}$
L	– Channel length, m
p	– Permeate
Q	– Flow rate, $l h^{-1}$
R	– Rejection ratio

r	– Retentate
Re	– Reynold number
S	– Membrane active area, m^2
Sc	– Schmidt number
Sh	– Sherwood number
u	– Flow velocity, $m s^{-1}$
w	– Width
Y	– Recovery rate
ν	– Kinematic viscosity of feed, $m^2 s^{-1}$
ΔP	– Difference operation pressure, bar
μ	– Dynamic viscosity, $Kg m^{-1} s^{-1}$
π	– Osmotic pressure, bar
ρ	– Density of the fluid, $Kg m^3$

References

- [1] G.M. Geise, H.S. Lee, D.J. Miller, B.D. Freeman, J.E. McGrath, D.R. Paul, Water purification by membrane: the role of polymer science, *J. Polym. Sci. Part B: Polym. Phys.*, 48 (2010) 1685–1718.
- [2] D. Johnson, N. Hilal, Characterisation and quantification of membrane surface properties using atomic force microscopy: a comprehensive review, *Desalination*, 356 (2015) 149–164.
- [3] K. Vairavamoorthy, S.D. Gorantiwar, A. Pathirana, Managing urban water supplies in developing countries climate change and water scarcity scenarios, *Phys. Chem. Earth.*, 33 (2008) 330–339.
- [4] N. Drouiche, N. Gaffer, M.W. Naceur, H. Lounici, M. Drouiche, Towards sustainable water management in Algeria, *Desal. Wat. Treat.*, 50 (2012) 272–284.
- [5] A. Almansoori, Y. Saif, Structural optimization of osmosis processes for water and power production in desalination application, *Desalination*, 344 (2014) 12–27.
- [6] S.B.E. Maliki, A. Benhabib, J. Charmes, Households poverty and water linkages: evidence from Algeria, 2009 Proceedings of the Middle East Economic Association J. of Middle East Economic Association and Loyola University Chicago, USA, 11 (2009) 1–27.
- [7] R. Mitiche, M. Metaiche, A. Kettab, F. Ammour, S. Otmani, S. Houli, S. Taleb, A. Maazouzi, Desalination in Algeria: current situation and development programs, *Desal. Wat. Treat.*, 14 (2010) 259–264.
- [8] H. Mahmoudi, N. Spahis, M.F. Goosen, N. Ghaffour, N. Drouiche, A. Ouagued, Application of geothermal energy for heating and fresh water production in a brackish water green house desalination: a case study from Algeria, *Renewable. Sustainable. Energy. Rev.*, 14 (2010) 512–517.
- [9] S. Subramani, R.C. Panda, Statistical regression and modelling analysis for reverse osmosis desalination process, *Desalination*, 351 (2014) 120–127.
- [10] D. Eisa Sachit, J.N. Veenstra, Analysis of reverse osmosis membrane performance during desalination of brackish surface waters, *J. Membr. Sci.*, 453 (2014) 136–154.
- [11] N. Ghaffour, T.M. Missimer, G.L. Amy, Technical review and evaluation of the economics of water desalination: current and future challenges for better water supply sustainability, *Desalination*, 309 (2013) 197–207.
- [12] Y. Wibisono, E.R. Cornelissen, A.J.B. Kemperman, W.G.J. Van der Meer, K. Nijmeijer, Two-phase flow in membrane processes: a technology with a future, *J. Membr. Sci.*, 453 (2014) 566–602.
- [13] D.K. Kohli, S. Bhartiya, A. Singh, R. Singh, M.K. Singh, P.K. Gupta, Capacitive deionization of ground water using carbon aerogel based electrodes, *Desal. Wat. Treat.*, 57 (2016) 26871–26879.
- [14] G. Vaseghi, A. Ghassemi, J. Loya, Characterization of reverse osmosis and nanofiltration membranes: effects of operating conditions and specific ion rejection, *Desal. Wat. Treat.*, 57 (2016) 23461–23472.
- [15] L.F. Greenlee, D.F. Lawler, B.D. Freeman, B. Marrot, P. Moulin, Reverse osmosis desalination: water sources, technology, and today's challenges, *Wat. Res.*, 43 (2009) 2317–2348.

- [16] S. Kimaru, S. Sourirajan, Analysis of data in reverse osmosis with porous cellulose acetate membrane, *AIChE J.*, 13 (1967) 497–503.
- [17] A.S. Michaels, New separation technique for the chemical process industries, *Chem. Eng. Progr.*, 64 (1968) 31–43.
- [18] K. Jamel, M.A. Khan, M. Kamil, Mathematical modelling of reverse osmosis systems, *Desalination*, 160 (2004) 29–42.
- [19] A. Rodríguez-Calvo, G.A. Silva-Castro, F. Osorio, J. González-López, C. Calvo, Reverse osmosis seawater desalination: current status of membrane systems, *Desal. Wat. Treat.*, 56 (2016) 849–861.
- [20] F.X. Kong, G.D. Sun, J.F. Chen, J.D. Han, C.M. Guo, T. Zhang, X.F. Lin, Y.F. Xie, Desalination and fouling of NF/low pressure RO membrane for shale gas fracturing flowback water treatment, *Sep. Purif. Technol.*, 195 (2018) 216–223.
- [21] T. Nguyen, F.A. Roddick, L. Fan, Biofouling of water treatment membranes: a review of the underlying causes, monitoring techniques and control measures, *Membranes*, 2 (2012) 804–840.
- [22] Filmtec™ Membranes - Filmtec TW30-2540 Tade water Reverse Osmosis Element, in, Dow Chemical Company, 2017.
- [23] G.M. Geise, H.B. Park, A.C. Sagle, B.D. Freeman, J.E. McGrath, Water permeability and water/salt selectivity trade off in polymers for desalination, *J. Membr. Sci.*, 369 (2011) 130–138.
- [24] K.P. Lee, T.C. Arnot, D. Matti, A review of reverse osmosis membrane materials for desalination—Development to date and future potential, *J. Membr. Sci.*, 370 (2011) 1–22.
- [25] T.Y. Qiu, P.A. Davies, Concentration polarization model of spiral-wound membrane modules with application to batch-mode RO desalination of brackish water, *Desalination*, 368 (2015) 36–47.
- [26] M. Taniguchi, S. Kimura, Estimation of transport parameters of RO membranes for seawater desalination, *AIChE J.*, 46 (2000) 1967–1973.
- [27] R.J. Petersen, Composite reverse osmosis and nanofiltration membranes, *J. Membr. Sci.*, 83 (1993) 81–95.

Appendix

Calculate of the mass transfer coefficient (k):

The mass transfer coefficients are [27]:

– laminar flow

$$k = 1.86(\mu.D^2 / dh.L)^{0.33} \quad (12)$$

– turbulent flow

$$k = 0.023(\mu^{0.8}.D^{0.67}) / (dh^{0.2}.v^{0.47}) \quad (13)$$

The density of water, the viscosity of the solution (water + salt), and the diffusivity of the salts in water are modelled at any point of the flow, depending on the temperature and concentration. It then accepts the following models according to [27]:

$$\rho_{(x,y)} \left(\frac{\text{kg}}{\text{m}^3} \right) = 498,4.m + \sqrt{248400.m^2 + 752,4.m.C_{(x,y)} \left(\frac{\text{kg}}{\text{m}^3} \right)} \quad (14)$$

with

$$m = 1,0069 - 2,757.10^{-4}.T(^{\circ}\text{C}) \quad (15)$$

$$\mu_{(x,y)} (\text{Pa.s}) = 1,234.10^{-6}.e^{\left[0,00212.C_{(x,y)} \left(\frac{\text{kg}}{\text{m}^3} \right) + \frac{1965}{273,15+T(^{\circ}\text{C})} \right]} \quad (16)$$

$$v_{(x,y)} \left(\frac{\text{m}^2}{\text{s}} \right) = \frac{\mu_{(x,y)} (\text{Pa.s})}{\rho_{(x,y)} \left(\frac{\text{kg}}{\text{m}^3} \right)} \quad (17)$$

$$D_{(x,y)} \left(\frac{\text{m}^2}{\text{s}} \right) = 6,725.10^{-6}.e^{\left[0,1546.10^{-3}.C_{(x,y)} \left(\frac{\text{kg}}{\text{m}^3} \right) - \frac{2513}{273,15+T(^{\circ}\text{C})} \right]} \quad (18)$$

$$u(m/s) = (Qf(m^3/s) / (2.h.w)) \quad (19)$$

with

h : feed channel height = 7.10×10^{-4} m; w : width = 1.3 m.

Calculate of the Sherwood number (Sh):

$$\text{Re} = (dh * u * \rho) / \mu \quad (20)$$

with

d_h = (2 × feed spacer thickness)
feed spacer thickness = 28 mm.

$$\text{Sc} = (\mu / \rho.D) \quad (21)$$